ACS APPLIED POLYMER MATERIALS

Open Access

pubs.acs.org/acsapm

Letter

Fluorine-Free Polynorbornene Membranes Based on a Sterically Hindered Pyridine for Vanadium Redox Flow Batteries

Julian Stonawski,* Frieder Junginger, Andreas Münchinger, Linus Hager, Simon Thiele, and Jochen Kerres*

Cite This: *ACS Appl. Polym. Mater.* 2024, 6, 13512−13517

Read Online

ACCESS | Metrics & More | Article Recommendations | Supporting Information

ABSTRACT: A 2,6-di-*tert*-butylpyridine-containing norbornene was synthesized by a one-step synthesis and copolymerized with an aromatic norbornene to obtain a membrane with a proton conductivity of 56 mS cm^{-1} in 2 M H_2SO_4. Decreased vanadium(IV) permeability was reached compared to the fluorine-containing reference membrane FAPQ330. A vanadium-(V) stability test for 55 days [1.6 M V(V)/2 M H_2SO_4] showed no degradation of functional groups but a loss of molecular weight. Vanadium redox flow battery single-cell tests resulted in a performance comparable to that of FAPQ330, and an in situ self-discharge test lasted more than 3 times longer for the cell equipped with pNorb-Pyr61.

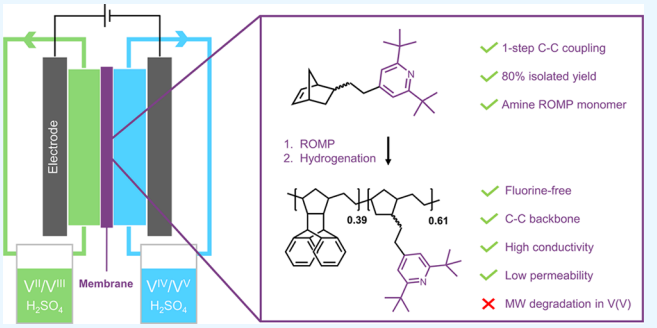

KEYWORDS: *ring-opening metathesis polymerization, polynorbornene, sterically hindered pyridine, ion-exchange membrane, vanadium redox flow battery*

The mitigation of greenhouse gas emissions demands the transition from conventional energy sources to renewable energy sources.[1] For this transition, the storage of fluctuating renewable energy sources, such as wind or solar energy, is required.[2] Among other systems, the vanadium redox flow battery (VRFB) is a promising technology for this purpose, which has already been demonstrated by the installation of several megawatt-scale projects in Japan and China.[3] In VRFBs, both electrode compartments are typically physically separated by a polymeric solid electrolyte membrane, which is intended to conduct ions, primarily protons, but prevent the crossover of vanadium-containing species.[4] Commercially available membranes, i.e., Nafion212 or FAPQ330, already show decent cell performances. However, both membranes contain fluorine, which is particularly problematic against the backdrop of a potential ban of per- and polyfluoroalkyl substances (PFAS) in the European Union and the potential impacts on human health by these substances.[5] For these reasons and to minimize the risk of the emission of PFAS into the environment, researchers are intensively searching for fluorine-free materials with comparable performances and stabilities.[6]

Ring-opening metathesis polymerization (ROMP) of norbornene-based monomers using Grubbs catalysts is a facile route to fluorine-free, mechanically stable, film-forming, and heteroatom-free polymers.[7] The straightforward preparation of norbornene monomers via a high-temperature Diels−Alder reaction between norbornadiene and the alkene with the respective functional group allows easy modification of the polymer's functionality, swelling properties, and mechanical properties.[8] For example, implementing bulky norbornenes increases T_g and reduces water uptake.[9] Based on this polymerization, several anion-exchange and cation-exchange materials have already been reported.[10,11] However, no application of polynorbornene-based materials in VRFB has been reported to date.

A series of VRFB membranes with neutral amines such as pyridines yielded superior performances and high stability against the V electrolyte, whereas for quaternized ammonium groups, degradation was reported.[12,13] However, ROMP catalysts suffer from limited functional group tolerance for coordinating amines, such as pyridines or alkylamines, which complicates the implementation of these functional groups prior to polymerization.[14] For example, only a few examples of ROMP polymers with free pyridine units were reported, which are either functionalized via an ester functionality that is likely to be unstable in an acidic environment,[15] contain fluorine,[16] or require a multistep monomer synthesis with low yield.[17] Hancock et al. reported an optimized synthesis route for a

Received: June 1, 2024
Revised: November 4, 2024
Accepted: November 4, 2024
Published: November 11, 2024

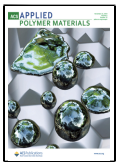

sterically hindered pyridine-containing monomer via cycloaddition of 2,3-pyridynes with cyclopentadiene, where the *tert*-butyl derivative showed the highest conversion and controllability in a subsequent ROMP. Considering the three-step synthesis of the monomer precursor, the total synthesis required six steps with an overall yield of 27% based on the starting materials ethyl formate and 3,3-dimethylbutan-2-one.[18]

Inspired by this work, we report the synthesis of a sterically hindered pyridine norbornene monomer via a one-step reaction between the commercially available 2,6-di-*tert*-butyl-4-methylpyridine and 5-(bromomethyl)bicyclo[2.2.1]hept-2-ene.[19] For this, anhydrous tetrahydrofuran (THF) and 2,6-di-*tert*-butyl-4-methylpyridine were placed into a Schlenk flask and cooled to −78 °C. Subsequently, 2,6-di-*tert*-butyl-4-methylpyridine was deprotonated by the addition of *sec*-butyllithium in cyclohexane/hexane and stirring for 1 h. Next, 5-(bromomethyl)bicyclo[2.2.1]hept-2-ene was added to the reaction flask, and the reaction mixture was allowed to reach room temperature (RT) overnight. After quenching with H_2O and purification by vacuum distillation, the monomer 4-[2-(bicyclo[2.2.1]hept-5-en-2-yl)ethyl]-2,6-di-*tert*-butylpyridine appeared as a clear, colorless oil. Compared to the above-mentioned synthesis of a sterically hindered pyridine-containing norbornene, the method is significantly simplified and showed an increased isolated yield of 80%.

A subsequent copolymerization with a bulky aromatic norbornene comonomer resulted in a polymer with excellent film-forming properties, which allowed for the efficient preparation of thin membranes. For this, 4-[2-(bicyclo[2.2.1]-hept-5-en-2-yl)ethyl]-2,6-di-*tert*-butylpyridine and (9*R*,10*S*,12*S*,13*S*,17*R*)-9,10-dihydro-9,10-[2]bicycloanthracene (for ^{1}H NMR, see Figure S10) were added to a Schlenk flask, dissolved in anhydrous dichloromethane, and polymerized by a Grubbs third-generation catalyst. The polymer was isolated, dried, and hydrogenated with *p*-toluenesulfonylhydrazide to yield Norb-Pyr61.

Subsequently, membranes prepared from Norb-Pyr61 were characterized by VRFB single-cell tests. At each current density of 50, 100, and 200 mA cm^{-2}, three constant current cycles were performed, within a state of charge (SOC) range of 20% and 80%. Afterward, a self-discharge test was performed by charging to an open-circuit voltage of 1.33 V (SOC = 20%) with a constant current of 20 mA cm^{-2}. After reaching SOC = 20%, the electrolyte flow was stopped to measure the battery cell voltage under static conditions until dropping to 0.9 V. A detailed description of all experimental details can be found in the Supporting Information.

A schematic representation of the synthesis of the sterically hindered pyridine norbornene monomer 4-[2-(bicyclo[2.2.1]-hept-5-en-2-yl)ethyl]-2,6-di-*tert*-butylpyridine is presented in Figure 1a.

Other groups have already reported the concept of using sterically hindered amines for ROMP.[18] However, synthesizing a pyridine-containing monomer required several steps with medium-to-low yields.[19] Our work expands the range of potential reaction partners of the deprotonated 2,6-di-*tert*-butyl-4-methylpyridine to unactivated alkyl bromides and provides access to a one-step synthesis of a sterically hindered free amine ROMP monomer with an isolated yield of 80% after distillation. The structure was confirmed by ^{1}H, ^{13}C, 2D-COSY, and 2D-HSQC NMR spectroscopy (Figures 2 and S1−S8).[20]

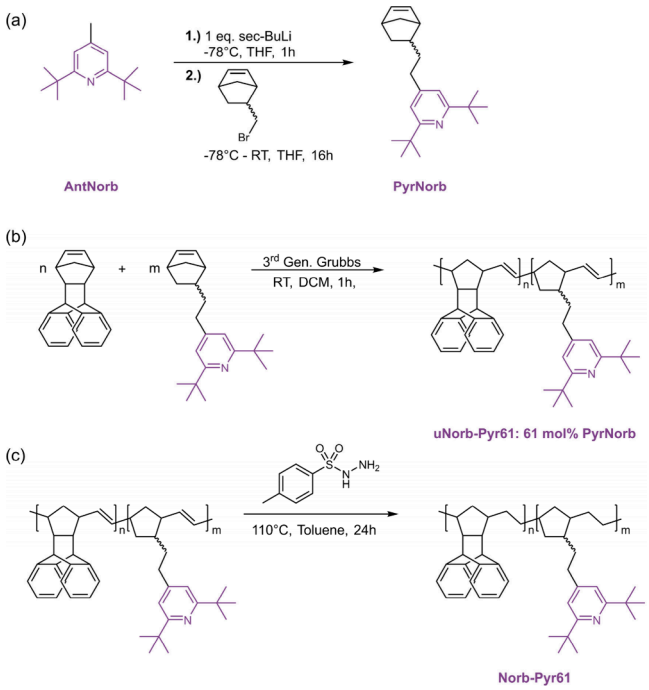

Figure 1. Schematic representation of the (a) monomer synthesis procedure, (b) polymerization procedure, and (c) hydrogenation of the polymer double bonds by tosylhydrazine. The wavy bond represents the possibility of endo and exo isomers.

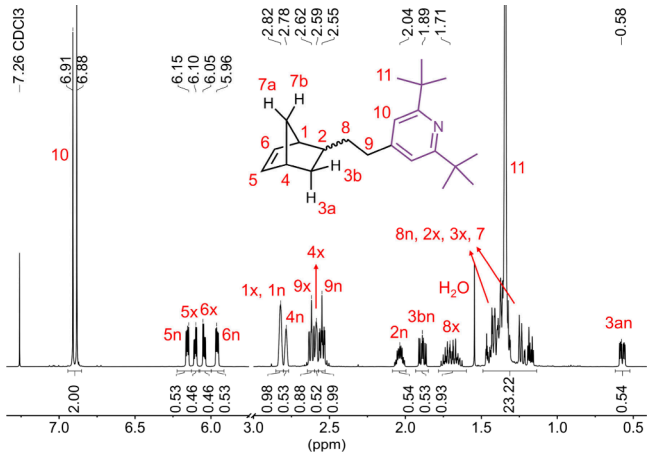

Figure 2. ^{1}H NMR spectrum of the isolated monomer. The region between 3 and 5.75 ppm was spared out for clarity. The complete ^{1}H NMR spectrum can be found in Figure S1. Protons assigned to the endo isomer are marked with n, and protons assigned to the exo isomer with x. The wavy bond represents the possibility of endo and exo isomers.

The endo/exo ratio was determined to be 54:46 by comparing the signals of the norbornene double bond in the range of 5.9−6.3 ppm, which is comparable to the endo/exo ratio found for commercially purchased 5-(bromomethyl)-bicyclo[2.2.1]hept-2-ene (Figure S9).[21,22]

The polymer synthesis is schematically represented in Figure 1b,c.[23] The choice of comonomer was made for several reasons: scalability and purification of the monomer, high T_g and sufficient mechanical properties, and reduced swelling of the corresponding polymer.[24] Norb-Pyr61 is soluble in aprotic solvents, such as chloroform, tetrahydrofuran, and dichloro-

https://doi.org/10.1021/acsapm.4c01686
ACS Appl. Polym. Mater. 2024, 6, 13512−13517

methane. The addition of sulfuric acid resulted in solubility in methanol and ethanol due to protonation of the pyridine moiety and an associated increase in hydrophilicity.

uNorb-Pyr61 and Norb-Pyr61 were analyzed by ^{1}H NMR (Figures S11–S13). After hydrogenation, no signals were observed in the vinylic proton region between 4.90 and 5.80 ppm, indicating the complete hydrogenation of all double bonds. By a comparison of the signals of the aromatic pyridine protons and the benzylic protons adjacent to the aromatic rings, the amount of pyridine-containing monomer was calculated to be 61 mol %, consistent with the monomer feed composition.

Size-exclusion chromatography (SEC) measurements of uNorb-Pyr61 in THF showed an M_n of 76000 g mol^{-1} and an M_w of 115000 g mol^{-1} ($Đ$ = 1.52), whereas for Norb-Pyr61, an M_n of 92000 g mol^{-1} and an M_w of 141000 g mol^{-1} ($Đ$ = 1.54) was measured (Figure S14), which allowed the preparation of free-standing and flexible films (Figure S17). Based on the catalyst/monomer ratio, a molecular weight of 66000 g mol^{-1} was expected. The higher measured molecular weights compared to the expected one and the difference between the saturated and unsaturated polymers can be explained by the different interactions of the polymers with THF, which can lead to different hydrodynamic radii and therefore to different results for M_n and M_w. Usually, ROMPs of norbornene derivatives proceed in a living fashion, leading to $Đ$ < 1.10.[25] However, the $Đ$ value is much higher than 1.10 in the present case. This observation could be due to the different reactivities of the endo and exo isomers of the monomer.[26] The thermal properties of the polymers were assessed by differential scanning calorimetry (DSC) and thermogravimetric analysis (TGA). The DSC measurement of unsaturated copolymer uNorb-Pyr61 showed a glass transition temperature of 125 °C, which was decreased to 102 °C after hydrogenation of the polymer (Figure S15). The TGA measurement showed high thermal stability with onset temperatures of 350 °C for uNorb-Pyr61 and 338 °C for Norb-Pyr61 (Figure S16).

Initially, the membrane was prepared in a deprotonated state. Surprisingly, no proton conductivity or swelling was observed when immersed in 2 M sulfuric acid, which is typically the case for other free amine-containing polymers.[27] This observation is probably due to the reduced protonation rate caused by the steric hindrance of the sterically hindered pyridine moiety.[28] To circumvent this problem, the polymer was protonated during the casting procedure. Adding 2 equiv of sulfuric acid based on the number of pyridine moieties to a Norb-Pyr61/ethanol mixture resulted in dissolution of the polymer and ensured complete protonation of the polymer. The resulting flexible membrane showed a proton conductivity of 56 mS cm^{-1} in 2 M sulfuric acid, slightly higher than the 38 mS cm^{-1} of the reference membrane FAPQ330 (Table 1).

Table 1. Overview of Ex Situ Properties of FAPQ330 and pNorb-Pyr61

membrane	thickness swelling (%)	ADL	σ^b (mS cm^{-1})
FAPQ330	29.6 ± 3.5	*a*	38 ± 3
pNorb-Pyr61	2.8 ± 1.5	1.1 ± 0.1	56 ± 1

[a]FAPQ330 turned black during back-titration in KOH. FUMATECH BWT GmbH does not provide any information on the chemical structure or ion-exchange capacity of the material, which does not allow the calculation of an ADL. [b]Through-plane in 2 M H_2SO_4.

Tensile tests were performed to assess the impact of the sulfuric acid addition on the mechanical properties of the resulting membrane (Figure S18–S20 and Table S1). As expected, excess sulfuric acid acts as a plasticizer, thus decreasing the tensile strength but increasing the flexibility of the membrane. Compared to FAPQ330, pNorb-Pyr61 is less flexible and cannot withstand similar tensile loads. However, the membranes were still mechanically tough enough to be easily handled and installed in the single-cell VRFB test setup without failure or punctuation.

The membranes were further characterized with respect to their swelling properties in 2 M sulfuric acid (Table 1). The acid doping level (ADL) is defined as the number of H_2SO_4 molecules per functional group, which in the case of pNorb-Pyr61 is the pyridine moiety. Immediately after membrane preparation, the theoretical ADL of pNorb-Pyr61 is 2 because 2 equiv of sulfuric acid, based on the number of pyridine groups, was added to the solution. However, after the membrane was immersed in 2 M H_2SO_4 for 48 h, the ADL is reduced to 1.1, meaning that each pyridine unit binds 1.1 H_2SO_4 molecules, 0.9 equiv of the initially present sulfuric acid has been washed out of the membrane, and almost no excess acid is stored inside the free volume of the membrane. The thickness swelling of the membranes is particularly important in constructing the cell because the initial swelling can introduce pressure-related forces to the system. As shown in Table 1, pNorb-Pyr61 exhibited almost no thickness swelling, an additional effect of sulfuric acid addition during the casting process.

The vanadium permeability of membranes significantly impacts the Coulombic efficiency (CE) and, therefore, the cycling life of a VRFB. The results of the ex situ V(IV) crossover tests for FAPQ330 and pNorb-Pyr61 are presented in Figure 3.

As can be seen in Figure 3a, the V(IV) concentration in the case of pNorb-Pyr61 rises significantly less compared to that of

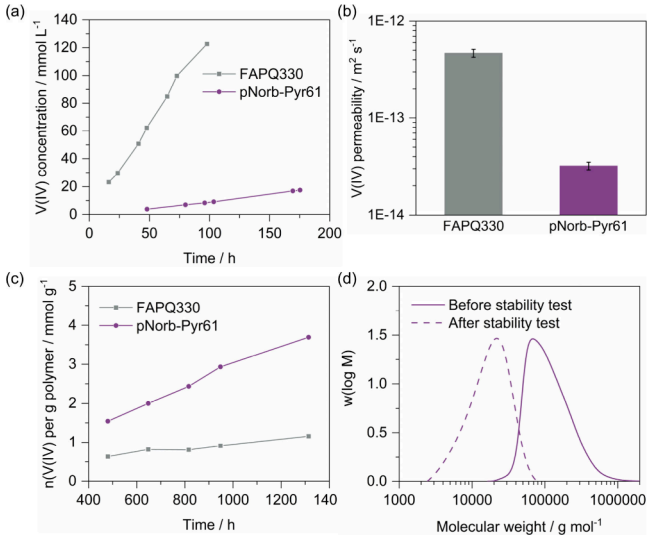

Figure 3. (a) V(IV) concentration over time of the tested membranes during the ex situ V(IV) permeability test. (b) V(IV) permeability of FAPQ330 and pNorb-Pyr61. (c) V(IV) evolution over time in the surrounding electrolyte for FAPQ330 and pNorb-Pyr61 during the stability test in 1.6 M V(V) in 2 M H_2SO_4 over 55 days. (d) Molecular weight distribution of pNorb-Pyr61 before and after the stability test.

https://doi.org/10.1021/acsapm.4c01686
ACS Appl. Polym. Mater. 2024, 6, 13512–13517

FAPQ330, which corresponds to a decreased ex situ V(IV) permeability (Figure 3b). This is probably a consequence of the above-mentioned low uptake of excess acid into the free volume.

In addition to V permeability, stability in the acidic V(V) electrolyte is another critical issue for battery lifetime. Stability tests were performed by immersing membrane pieces in the fully charged electrolyte containing 1.6 M V(V) in 2 M H_2SO_4 for 55 days. The V(IV) concentration in the case of the pNorb-Pyr61 sample increased significantly faster than that of FAPQ330, indicating a faster reaction of V(V) with the polymer (Figure 3c). SEC and ^{1}H NMR measurements of the polymer were performed before and after the stability test to evaluate this degradation further. A comparison of the ^{1}H NMR spectra showed no evidence of functional group degradation (Figure S21). However, as shown in Figure 3d, the molecular weight of the polymer decreased from M_n = 92.000 to 14.000 g mol^{-1}, resulting in mechanical disintegration of the membrane pieces. The molecular structure of Norb-Pyr61 in Figure 1 only allows for molecular weight degradation through C−C bond cleavage. To our knowledge, no such C−C bond cleavage has ever been reported for VRFBs. However, analyzing the underlying mechanisms for the polymer backbone degradation would require considerable experimental effort, which is beyond the scope of this paper and will be the subject of future studies.

On the basis of the promising ex-situ results, we further characterized the material in a VRFB single-cell test for three cycles, each at 50, 100, and 200 mA cm^{-2} and in a static in situ self-discharge test. The corresponding results are shown in Figure 4.

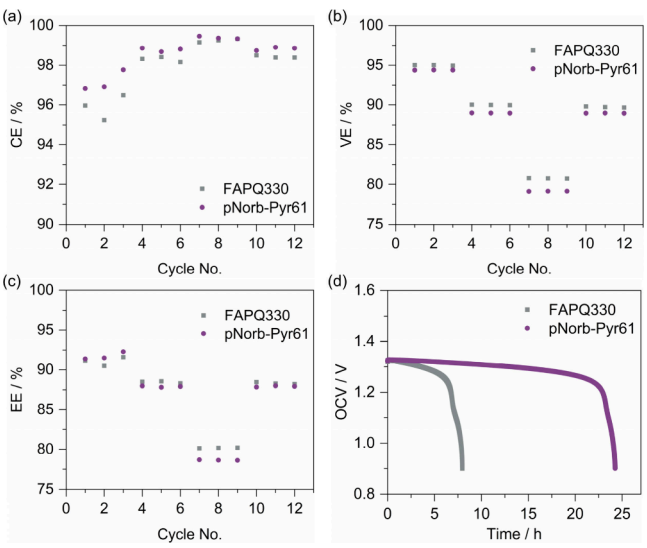

Figure 4. (a) CE, (b) VE, and (c) EE of a VRFB single cell equipped with FAPQ330 and pNorb-Pyr61 at 50, 100, and 200 mA cm^{-2}. (d) In situ static self-discharge test of FAPQ330 and pNorb-Pyr61.

Three cycles were performed at each current density (50, 100, and 200 mA cm^{-2}). The averages of these three cycles and the corresponding standard deviations are listed in Table S2. As shown in Figure 4a, the CE generally increases with higher current densities for both cells tested due to reduced charge and discharge times. Especially at low current densities, a slightly higher CE was observed for pNorb-Pyr61 (98.8% at 100 mA cm^{-2}) compared to FAPQ330 (98.3% at 100 mA cm^{-2}), which is consistent with the more than 3 times longer self-discharge time shown in Figure 4d and the lower ex situ V(IV) permeability shown in Figure 3b for pNorb-Pyr61. Thus, the above-mentioned material design concept utilizing free amines and a bulky hydrophobic comonomer is also reflected in the cell self-discharge performance because a decreased swelling is connected to a reduced V crossover. In terms of voltage efficiency (VE), the cell equipped with pNorb-Pyr61 showed slightly lower VE (89.0%) than the cell equipped with FAPQ330 (90.0%) at a current density of 100 mA cm^{-2}, which is mainly a result of higher area specific resistance (ASR) due to the slightly greater thickness of pNorb-Pyr61 (35 μm) compared to FAPQ330 (30 μm) (Figure 4b). The energy efficiency (EE) is the product of VE and CE. At low current densities (<50 mA cm^{-2}), the EE is dominated by the CE, while at high current densities (>200 mA cm^{-2}), the EE is mainly governed by the ohmic losses, i.e., the VE.[29] Moderate current densities (100 mA cm^{-2}) represent a kind of inflection point where the performance of pNorb-Pyr61 (EE = 87.9%) virtually matches that of FAPQ330 (EE = 88.5%) (Figure 4c). To summarize the VRFB single-cell test results, both membranes showed comparable performance in terms of efficiency, with the cell equipped with pNorb-Pyr61 having a better crossover performance but also slightly higher ASR than FAPQ330.

CONCLUSION

In conclusion, a sterically hindered, fluorine-free, and pyridine-containing norbornene monomer was prepared via an efficient one-step C−C coupling reaction of two commercially available starting materials with an improved isolated yield of 80%. The chemical structure of the monomer was confirmed, and the steric hindrance of the pyridine moiety allowed a successful ROMP with a bulky aromatic comonomer. The innovative material design led to sufficient mechanical properties, allowing flexible membranes with high ex situ proton conductivity to be prepared. Swelling tests showed that almost no excess acid is stored in the free volume of the polymer structure. Ex situ V(IV) permeability tests revealed significantly improved V(IV) permeability properties compared with the reference membrane FAPQ330, while the V(V) stability test revealed backbone degradation, resulting in a molecular weight reduction.

An in situ VRFB single-cell test demonstrated the general applicability of the membrane with results comparable to those of a commercially available fluorine-containing membrane. An in situ static self-discharge test lasted more than 3 times longer than that of FAPQ330, resulting from the high hydrophobicity of the bulky norbornene and the sterically hindered pyridine. Future research should especially analyze the underlying mechanism of polymer backbone degradation to enable the development of fluorine-free materials with improved chemical stability.

ASSOCIATED CONTENT

Supporting Information

The Supporting Information is available free of charge at https://pubs.acs.org/doi/10.1021/acsapm.4c01686.

Additional spectroscopic, DSC, and TGA data (PDF)

https://doi.org/10.1021/acsapm.4c01686
ACS Appl. Polym. Mater. 2024, 6, 13512−13517

AUTHOR INFORMATION

Corresponding Authors

Julian Stonawski − *Helmholtz-Institute Erlangen-Nürnberg for Renewable Energy (IET-2), Forschungszentrum Jülich GmbH, 91058 Erlangen, Germany; Department of Chemical and Biological Engineering, Friedrich-Alexander-Universität Erlangen-Nürnberg, 91058 Erlangen, Germany;* orcid.org/0009-0003-0062-9925; Email: j.stonawski@fz-juelich.de, stonawski.julian@web.de

Jochen Kerres − *Helmholtz-Institute Erlangen-Nürnberg for Renewable Energy (IET-2), Forschungszentrum Jülich GmbH, 91058 Erlangen, Germany; Faculty of Natural Science, North-West University, Potchefstroom 2520, South Africa;* orcid.org/0000-0003-4972-6307; Email: j.kerres@fz-juelich.de

Authors

Frieder Junginger − *Electrochemical Energy Systems, IMTEK—Department of Microsystems Engineering, University of Freiburg, 79110 Freiburg, Germany*

Andreas Münchinger − *Electrochemical Energy Systems, IMTEK—Department of Microsystems Engineering, University of Freiburg, 79110 Freiburg, Germany*

Linus Hager − *Helmholtz-Institute Erlangen-Nürnberg for Renewable Energy (IET-2), Forschungszentrum Jülich GmbH, 91058 Erlangen, Germany; Department of Chemical and Biological Engineering, Friedrich-Alexander-Universität Erlangen-Nürnberg, 91058 Erlangen, Germany*

Simon Thiele − *Helmholtz-Institute Erlangen-Nürnberg for Renewable Energy (IET-2), Forschungszentrum Jülich GmbH, 91058 Erlangen, Germany; Department of Chemical and Biological Engineering, Friedrich-Alexander-Universität Erlangen-Nürnberg, 91058 Erlangen, Germany;* orcid.org/0000-0002-4248-2752

Complete contact information is available at: https://pubs.acs.org/10.1021/acsapm.4c01686

Author Contributions

J.S.: conceptualization, methodology, investigation, data curation, visualization, and writing—original draft. F.J.: investigation and writing—review and editing. A.M.: writing—review and editing. L.H.: investigation and writing—review and editing. S.T.: supervision and writing—review and editing. J.K.: supervision, conceptualization, writing—review and editing, and funding acquisition.

Funding

This project has been funded by the German Federal Ministry for Economic Affairs and Climate Action (BMWK, No. 03EI3018B).

Notes

The authors declare no competing financial interest.

REFERENCES

(1) Harichandan, S.; Kar, S. K.; Bansal, R.; Mishra, S. K.; Balathanigaimani, M. S.; Dash, M. Energy transition research: A bibliometric mapping of current findings and direction for future research. *Cleaner Prod. Lett.* **2022**, *3*, 100026.

(2) Kittel, M.; Schill, W.-P. Renewable energy targets and unintended storage cycling: Implications for energy modeling. *iScience* **2022**, *25* (4), 104002.

(3) Kear, G.; Shah, A. A.; Walsh, F. C. Development of the all-vanadium redox flow battery for energy storage: a review of technological, financial and policy aspects. *Int. J. Energy Res.* **2012**, *36* (11), 1105−1120.

(4) Tempelman, C.; Jacobs, J. F.; Balzer, R. M.; Degirmenci, V. Membranes for all vanadium redox flow batteries. *J. Energy Storage* **2020**, *32*, 101754.

(5) European Chemicals Agency. *ANNEX XV Restriction Report.* https://echa.europa.eu/de/restrictions-under-consideration/-/substance-rev/72301/term (accessed 2024-05-01).

(6) Miyake, J.; Miyatake, K. Fluorine-free sulfonated aromatic polymers as proton exchange membranes. *Polym. J.* **2017**, *49* (6), 487−495.

(7) Slugovc, C. The Ring Opening Metathesis Polymerisation Toolbox. *Macromol. Rapid Commun.* **2004**, *25* (14), 1283−1297.

(8) Martínez-Arranz, S.; Albéniz, A. C.; Espinet, P. Versatile Route to Functionalized Vinylic Addition Polynorbornenes. *Macromolecules* **2010**, *43* (18), 7482−7487.

(9) Cao, D.; Yang, F.; Sheng, W.; Zhou, Y.; Zhou, X.; Lu, Y.; Nie, F.; Li, N.; Pan, L.; Li, Y. Polynorbornene-based anion exchange membranes with hydrophobic large steric hindrance arylene substituent. *J. Membr. Sci.* **2022**, *641*, 119938.

(10) He, Z.; Wang, G.; Wang, C.; Guo, L.; Wei, R.; Song, G.; Pan, D.; Das, R.; Naik, N.; Hu, Z.; Guo, Z. Overview of Anion Exchange Membranes Based on Ring Opening Metathesis Polymerization (ROMP). *Polym. Rev.* **2021**, *61* (4), 689−713.

(11) Santiago, A. A.; Vargas, J.; Tlenkopatchev, M. A.; López-González, M.; Riande, E. Ion-Exchange Membranes Based on Polynorbornenes with Fluorinated Imide Side Chain Groups. *Int. J. Chem. Eng.* **2012**, *2012*, 1−11.

(12) Mu, T.; Tang, W.; Jin, Y.; Che, X.; Liu, J.; Yang, J. Ether-Free Poly(p -terphenyl- co -acetylpyridine) Membranes with Different Thicknesses for Vanadium Redox Flow Batteries. *ACS Appl. Energy Mater.* **2022**, *5* (9), 11713−11722.

(13) Hao, X.; Chen, N.; Chen, Y.; Chen, D. Accelerated degradation of quaternary ammonium functionalized anion exchange membrane in catholyte of vanadium redox flow battery. *Polym. Degrad. Stab.* **2022**, *197*, 109864.

(14) Takano, S.; Tamegai, H.; Itoh, T.; Ogata, S.; Fujimori, H.; Ogawa, S.; Iida, T.; Wakatsuki, Y. ROMP polymer-based antimicrobial films repeatedly chargeable with silver ions. *React. Funct. Polym.* **2011**, *71* (2), 195−203.

(15) Buchmeiser, M. R.; Lubbad, S.; Mayr, M.; Wurst, K. Access to silica- and monolithic polymer supported C-C-coupling catalysts via ROMP: applications in high-throughput screening, reactor technology and biphasic catalysis. *Inorg. Chim. Acta* **2003**, *345*, 145−153.

(16) Houck, M. B.; Fuhrer, T. J.; Phelps, C. R.; Brown, L. C.; Iacono, S. T. Toward Taming the Chemical Reversibility of Perfluoropyridine through Molecular Design with Applications to Pre- and Postmodifiable Polymer Architectures. *Macromolecules* **2021**, *54* (12), 5586−5594.

(17) Tanida, H.; Irie, T. Neighboring group participation by pyridine ring. 3. Synthesis and solvolysis of 5,8-dihydro- and 5,6,7,8-tetrahydro-5,8-methanoquinoline derivatives. *J. Org. Chem.* **1987**, *52* (23), 5218−5224.

(18) Hancock, S. N.; Yuntawattana, N.; Valdez, S. M.; Michaudel, Q. Expedient Synthesis and Ring-Opening Metathesis Polymerization of Pyridinonorbornenes. *Polymer chemistry* **2022**, *13* (39), 5530−5535.

(19) Wright, M. E.; Pulley, S. R. An improved synthesis of 4-vinyl-2,6-di-tert-butylpyridine and its suspension copolymerization with styrene and divinylbenzene. *J. Org. Chem.* **1987**, *52* (8), 1623−1624.

(20) Fisher, J.; Gradwell, M. J. Complete assignment of the 1 H and 13 C NMR spectra of norbornene derivatives. *Magn. Reson. Chem.* **1991**, *29* (10), 1068−1069.

(21) Laszlo, P.; Schleyer, P. v. R. Analysis of the Nuclear, Magnetic Resonance Spectra of Norbornene Derivatives. *J. Am. Chem. Soc.* **1964**, *86* (6), 1171−1179.

(22) Müller, K.; Chun, S.-H.; Greiner, A.; Agarwal, S. 2D NMR characterisation of 5-norbornene-2-nonaneacidethylester and 5-norbornene-2-hexane. *Des. Monomers Polym.* **2005**, *8* (3), 237−248.

(23) Sohn, B. H.; Gratt, J. A.; Lee, J. K.; Cohen, R. E. Hydrogenation of ring opening metathesis polymerization polymers. *J. Appl. Polym. Sci.* **1995**, *58* (6), 1041−1046.
(24) Cui, J.; Yang, J.-X.; Pan, L.; Li, Y.-S. Synthesis of Novel Cyclic Olefin Polymer with High Glass Transition Temperature via Ring-Opening Metathesis Polymerization. *Macromol. Chem. Phys.* **2016**, *217* (24), 2708−2716.
(25) Bielawski, C. W.; Grubbs, R. H. Living ring-opening metathesis polymerization. *Prog. Polym. Sci.* **2007**, *32* (1), 1−29.
(26) Nishihara, Y.; Inoue, Y.; Nakayama, Y.; Shiono, T.; Takagi, K. Comparative Reactivity of Exo - and Endo -Isomers in the Ru-Initiated Ring-Opening Metathesis Polymerization of Doubly Functionalized Norbornenes with Both Cyano and Ester Groups. *Macromolecules* **2006**, *39* (22), 7458−7460.
(27) Kennemur, J. G. Poly(vinylpyridine) Segments in Block Copolymers: Synthesis, Self-Assembly, and Versatility. *Macromolecules* **2019**, *52* (4), 1354−1370.
(28) Bernasconi, C. F.; Carre, D. J. Rate of protonation of 2,6-di-tert-butylpyridine by the hydronium ion. Steric hindrance to proton transfer. *J. Am. Chem. Soc.* **1979**, *101* (10), 2707−2709.
(29) Kreuer, K.-D.; Münchinger, A. Fast and Selective Ionic Transport: From Ion-Conducting Channels to Ion Exchange Membranes for Flow Batteries. *Annu. Rev. Mater. Res.* **2021**, *51* (1), 21−46.

https://doi.org/10.1021/acsapm.4c01686
ACS Appl. Polym. Mater. 2024, 6, 13512−13517